Journal of Molecular Graphics and Modelling 42 (2013) 73–80

Contents lists available at SciVerse ScienceDirect

Journal of Molecular Graphics and Modelling

journal homepage: www.elsevier.com/locate/JMGM

Modeling of the energies and splitting of the Q_x and Q_y bands in positional isomers of zinc pyridinoporphyrazines by TDDFT approach: Can TDDFT help distinguishing the structural isomers?

Yunling Gao[a,b], Victor N. Nemykin[a,*]

[a] Department of Chemistry and Biochemistry, University of Minnesota-Duluth, Duluth, MN 55812, United States
[b] State Key Laboratory Breeding Base of Green Chemistry Synthesis Technology, College of Chemical Engineering & Materials Science, Zhejiang University of Technology, Hangzhou 310032, China

ARTICLE INFO

Article history:
Accepted 8 March 2013
Available online 15 March 2013

Keywords:
Pyridinoporphyrazines
DFT
TDDFT
UV–vis spectra
Phthalocyanines

ABSTRACT

Electronic structures, energies and splitting of the Q_x and Q_y bands for positional isomers of zinc mono-, di-, tri-, and tetra pyridinoporphyrazines as well as parent zinc phthalocyanine were investigated using density functional theory (DFT) and time-dependent (TD) DFT approaches. The influence of the Hartree–Fock exchange on excited state energies and Q_x and Q_y bands splitting were studied using GGA BP86 and hybrid B3LYP and PBE1PBE exchange-correlation functionals. Solvent effects were estimated using the polarized continuum model (PCM) approach and cyclohexane, toluene, or DMSO as solvents. It was found that general trends in the Q_x and Q_y band energies and splitting correlate very well with the available experimental data on pyridinoporphyrazines and follow the trends in HOMO–LUMO and HOMO–LUMO + 1 energy gaps as well as LUMO–LUMO + 1 splitting. TDDFT trends allow estimation of the Q_x and Q_y band energies and splitting in unknown tripyridinoporphyrazines and in individual positional isomers of tetrapyridinoporphyrazines.

1. Introduction

Phthalocyanines (Pcs) [1–5] have recently attracted considerable attention as active components in semiconductor devices [2], molecular electronics [3], nonlinear optics [4], and photodynamic therapy of cancer [5] because of their simple synthesis, high stability, and unique absorption spectra. The pyridinoporphyrazines [6–11] are heterocyclic analogues of the phthalocyanines, in which benzene fragments are replaced with one or more of the electron-withdrawing pyridine rings. The pyridinoporphyrazines show similar to Pcs UV–vis absorption spectra with the Soret- and *Q*-bands slightly shifted to the higher energy. Substitution of the benzene rings in Pcs by the electron-withdrawing pyridine fragment(s) results in stabilization of the HOMO and therefore pyridinoporphyrazines have higher stability toward oxidants. The introduction of the pyridine rings also allows for easy quaternization, which can modulate the solubility of Pc analogues in aqueous media. Moreover, these water-soluble Pcs analogues do not form aggregates in aqueous solutions. Because of the above characteristics, the pyridinoporphyrazines have received more attention in potential application as electron or energy transfer agents [12], photosensitizers for photodynamic therapy [13], DNA binders [14] and catalysts [15].

The first pyridinoporphyrazines [16], tetrapyridinoporphyrazines (as a mixture of positional isomers **12**–**15**, Fig. 1) in which, four outer benzene rings are replaced by pyridine fragments, were synthesized by Linstead et al. in 1937 using standard condensation of 3,4-dicyanopyridine. Yokote et al. [17–19] have reported the application of unsubstituted benzopyridoporphyrazines as dye and the compounds containing a mixture of benzenoid and pyridinoid rings by condensation of pyridine carboxylic acid anhydride and phthalic anhydride. Hanack [20], Tokita [21], Sakamoto et al. [22] have synthesized variety of asymmetric benzopyridoporphyrazines derivatives. In all cases [16–24], pyridinoporphyrazines were isolated as a mixture of positional isomers. Sakamoto et al. [25] used the 'sulfuric acid soluble' method to separate the positional isomers of copper dibenzodipyridoporphyrazine **4**–**7** (Fig. 1) for the first time. In 2001, Sakamoto et al. [25] have also reported synthesis, optical spectroscopy, fluorescence, and cyclic voltammetry data on positional isomers of zinc dibenzo-di(3,4-pyrido)porphyrazines **4**–**7**. Cook [26], Kobayashi et al. [27] have studied the photophysical properties of tri-*tert*-butylpyridinotribenzotetraazaporphinato zinc **2** (ZnPcPy) and a self-assembled dimer of ZnPcPy in a non-polar solvent. In general, when two or more benzene rings are replaced by pyridine rings, the prepared pyridinoporphyrazine analogues are represented as a mixture of positional isomers. These positional isomers have

* Corresponding author.
E-mail address: vnemykin@d.umn.edu (V.N. Nemykin).

1093-3263/$ – see front matter © 2013 Elsevier Inc. All rights reserved.
http://dx.doi.org/10.1016/j.jmgm.2013.03.002

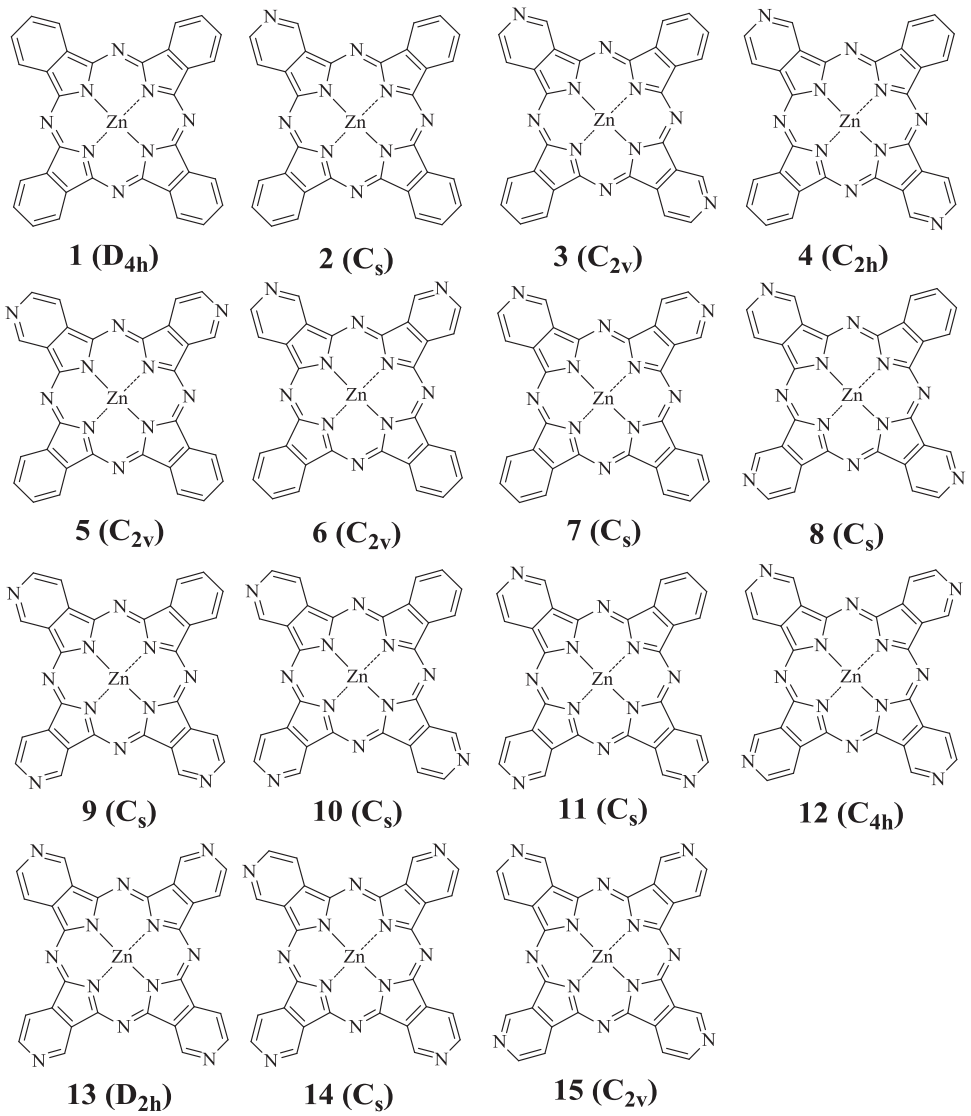

Fig. 1. Zinc phthalocyanine (**1**) and its pyridinoporphyrazine analogues (**2**–**15**).

the same molecular weight and close spectral properties, which makes their individual identification by standard methods quite challenging.

UV–vis spectra of phthalocyanines and their analogues are usually explained based on Gouterman's classic four-orbital model [28–32], that is, the energetically well-separated HOMO and HOMO − 1 and the degenerate or nearly degenerate LUMO and LUMO + 1 are predominantly responsible for their Soret and *Q* band absorptions. The transitions from $a_{1u} \rightarrow e_g(y)$ and $a_{2u} \rightarrow e_g(x)$ have *x*-polarization (in standard D_{4h} point group notation), while excited states from $a_{1u} \rightarrow e_g(x)$ and $a_{2u} \rightarrow e_g(y)$ have *y*-polarization. Both *x* and *y*-polarization transitions are further mixed and split in energy and create higher energy B_x and B_y transitions, and lower energy Q_x and Q_y transitions (Fig. 2). In the simplest case of D_{4h} symmetry ZnPc, because of the large energy difference between a_{1u} (HOMO) and a_{2u} (HOMO − 1) the *Q*-band often extrapolated as an almost pure single electron transition from HOMO (a_{1u}) to doubly degenerate LUMO and LUMO + 1 orbitals (Fig. 2). When one of benzene fragments in **1** is substituted by a pyridine ring, the effective symmetry of **2** (C_s) lifts the degeneracy of the LUMO and LUMO + 1, resulting in splitting of the Q_x and Q_y bands (Fig. 2). Similarly, pyridinoporphyrazines with effective symmetries of D_{2h}, C_{2v}, C_{2h} and C_s (compounds **3**–**11** and **13**–**15**, Fig. 1) should have split Q_x and Q_y bands in their UV–vis spectra, while pyridinoporphyrazine **12** should have degenerate LUMO and LUMO + 1 and thus a single *Q*-band. The degree of splitting and energies of the Q_x and Q_y band positions in pyridinoporphyrazines are not easy to predict using simple empirical methods and thus, assignments of the individual isomers in pyridinoporphyrazines until now were based on intuitive approach [25–27]. Since modern DFT and TDDFT methods have been successfully used to accurately predict the optical properties of phthalocyanines and their analogues [33–36], it was tempting for us to correlate known spectroscopic signatures of the individual isomers of pyridinoporphyrazines (Fig. 1) with those predicted by theoretical methods, as well as attempt to predict the spectroscopic properties of the individual isomers of pyridinoporphyrazines **8**–**15**, which experimental UV–vis properties remain unexplored. In this report, such spectroscopic characteristics of pyridinoporphyrazines **2**–**15** were modeled by TDDFT methods using three different exchange-correlation functionals (PBE1PBE, B3LYP, and BP86) in both vacuum and different solvents.

2. Experimental

The spectra of individual positional isomers of pyridinoporphyrazines were obtained from Prof. Keichii Sakamoto, Prof.

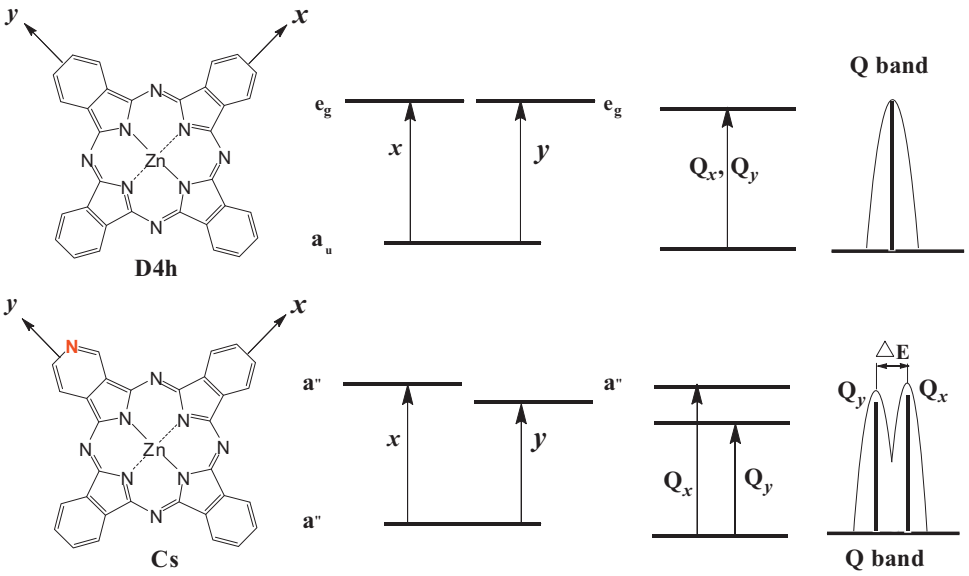

Fig. 2. Simplified Gouterman's four-orbital model for Q-band region of zinc pthalocyanine (**1**), and zinc monopyridinoporphyrazine (**2**).

Eugenii Lukyanets or adapted from the available literature sources [25,27,37].

2.1. Computational aspects

The molecular geometries were obtained either in the vacuum or in cyclohexane, toluene, and DMSO via optimization with hybrid Becke [38] three-parameters exchange functional and the Lee–Yang–Parr [39] nonlocal correlation functional (B3LYP, 20% of Hartree–Fock exchange), Perdew, Burke, and Ernzerhof's exchange functional along with their 1996 gradient-corrected correlation functional [40,41] (PBE1PBE, 25% of Hartree–Fock exchange) and Becke's [42] pure exchange and Perdew's [43] correlation GGA functional BP86 (0% of Hartree–Fock exchange). We used these three exchange-correlation functionals in order to investigate the influence of the Hartree–Fock exchange on the calculated vertical excitation energies of the pyridinoporphyrazines. The 6-31G [44] basis set for zinc and the 6-31G(d) [45] basis set for all atoms were used for all calculations. The equilibrium geometries were confirmed by the absence of the imaginary frequencies. Solvation effects were modeled using PCM [46] approach. TDDFT calculations were conducted using PBE1PBE, B3LYP, and BP86 functionals in vacuum, cyclohexane, toluene, and DMSO. The first forty excited states were calculated using non-equilibrium PCM solvation methods. All DFT calculations were carried out using the Gaussian 09 [47] software package running under a UNIX OS.

3. Results and discussion

3.1. Electronic structure of pyridinoporphyrazines 2–15

The frontier molecular orbitals of ZnPc **1** and the other fourteen pyridinoporphyrazines analogues are shown in Figs. 3 and S1–S13 and their shapes were found to be virtually independent from used exchange-correlation functional. As expected, DFT calculations predict that the LUMO and LUMO + 1 in compounds **1** and **12** are degenerate e_g MOs, while the HOMO has a_{1u} and a_u symmetries, respectively. Although degeneracy is lifted to some extent for the LUMO and LUMO + 1 in the case of pyridinoporphyrazines **2**–**11** and **13**–**15**, their shapes resemble the e_g set observed in **1** and **12**. Interestingly, the LUMO and LUMO + 1 are nearly degenerate in the case of pyridinoporphyrazines **7** and **15** despite their low symmetries. Similarly, the HOMO has a very similar shape in all tested compounds and resembles the a_{1u} MO of the parent phthalocyanine **1**.

Taking into consideration our target for accurate prediction of the energies and splittings of Q_x and Q_y bands in pyridinoporphyrazines **2**–**15**, we first explored the effect of Hartree Fock exchange present in different exchange-correlation functionals on the energies of HOMO, LUMO, and LUMO + 1 calculated in the vacuum and different solvents. As shown for a typical example in Figs. 4 and S1–S13, the energies of the HOMO gradually decrease, while the energies of the LUMO gradually increase with an increase of the Hartree–Fock exchange present in the corresponding exchange-correlation functional (0% in BP86, 20% in B3LYP, and 25% in PBE1PBE). As a result, the HOMO–LUMO energy gap also increases with the increase of the Hartree–Fock exchange presented in the exchange-correlation functional, which is typical for a DFT approach [29,33]. A smaller HOMO–LUMO energy gap for the BP86 functional would result in lower calculated Q_x- and Q_y-bands energies compared to those predicted using B3LYP and PBE1PBE exchange-correlation functionals. It can be clearly seen from Fig. 4 and Figs. S1–S13 that the gradual increase of the solvent

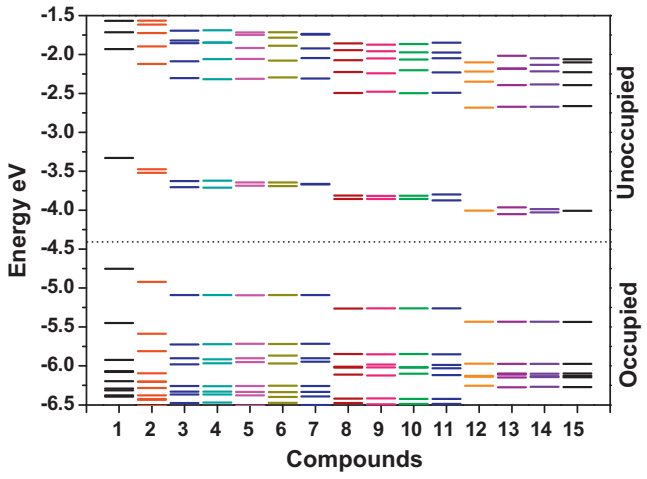

Fig. 3. DFT predicted orbital energies for compounds **1**–**15** calculated using BP86 exchange-correlation functional in vacuum.

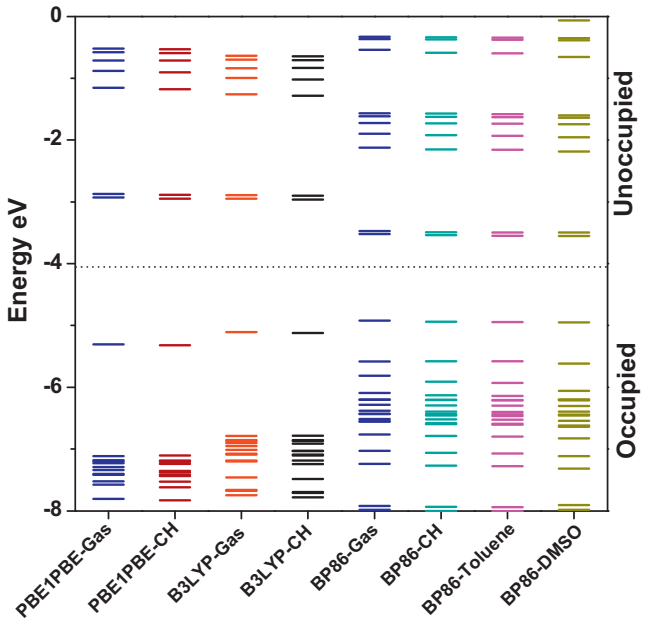

Fig. 4. DFT predicted orbital energies of compound **2** calculated using PBE1PBE, B3LYP, and BP86 functionals in vacuum and solvents (cyclohexane is abbreviated as CH).

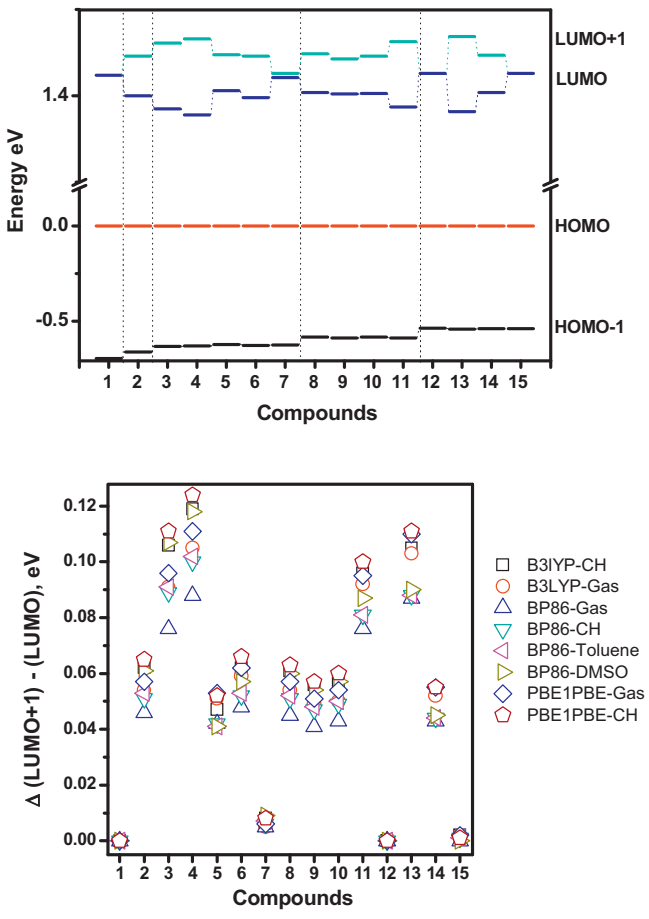

Fig. 5. DFT predicted HOMO, HOMO − 1, LUMO, and LUMO + 1 of compounds **1**–**15** calculated using BP86 exchange-correlation functional in vacuum. The HOMO energy is normalized to 0 eV (top); DFT predicted energy gap between LUMO and LUMO + 1 for compounds **1**–**15** using PBE1PBE, B3LYP, and BP86 functionals (bottom) Cyclohexane is abbreviated as CH.

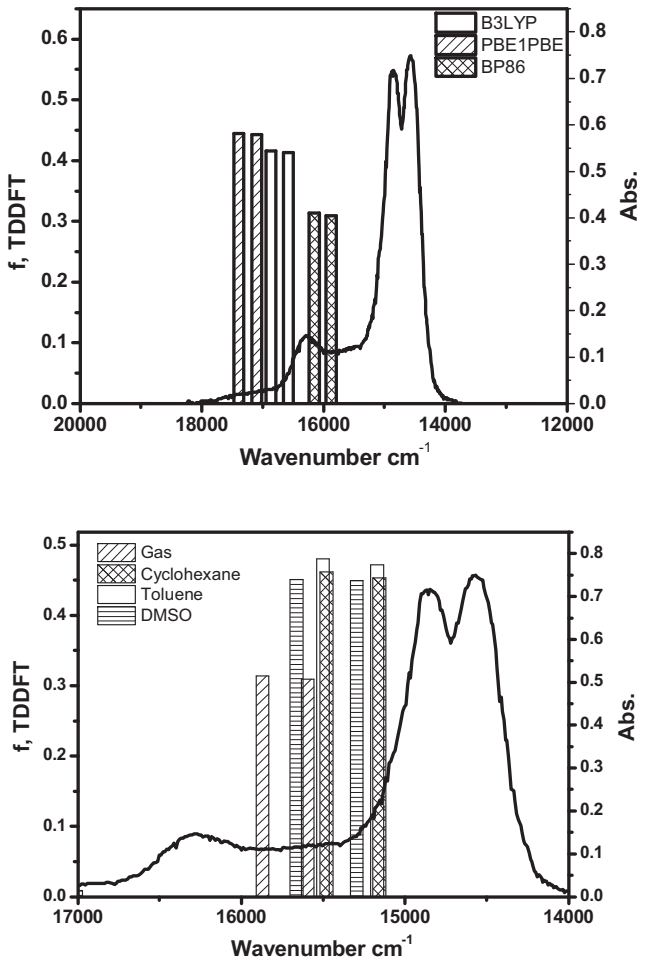

Fig. 6. Experimental UV–vis spectra of *Q*-band region and TDDFT-predicted vertical excitation energies using PBE1PBE, B3LYP, and BP86 exchange-correlation functionals in vacuum (top) and different solvents (BP86 functional only, bottom) for compound **2**.

polarity has only very minor influence on the calculated energies of HOMO, LUMO, and LUMO + 1 when the same exchange-correlation functional was used for the DFT calculations. Both HOMO and LUMO increase their stability as polarity of the solvent increases, but such stabilization has only ~0.1 eV magnitude.

Similar to the case of symmetric phthalocyanine compounds, the HOMO, LUMO, and LUMO + 1 in compounds **1**–**15** are energetically well separated from other MOs (Figs. 4 and S1–S13). The stepwise introduction of the pyridine substituents in the phthalocyanine core results in stabilization of corresponding HOMO and LUMO. It is interesting to note that such stabilization is rather sequential. From Fig. 3, it is obvious that stabilization of the HOMO is mostly, if not entirely, sensitive only to the number of nitrogen atoms present in corresponding pyridinoporphyrazine. This observation can be explain on the basis of the HOMO shape. Indeed, the HOMO in compounds **1**–**15** is strongly delocalized over the macrocycle with significant contribution originating from the peripheral pyridine-type nitrogen atom(s).

Overall, the DFT-predicted energy separation between the LUMO and LUMO + 1 in compounds **1**–**15** can provide an initial insight into the Q_x and Q_y bands splitting and help with the assignment of the individual structural isomers of pyridinoporphyrazines. For instance, because of the degeneracy or nearly degeneracy of the LUMO and LUMO + 1 in compounds **12** and **15** their *Q*-band region should be similar to the ZnPc **1** with non-splitted *Q*-band, while the other isomers may have splitted Q_x

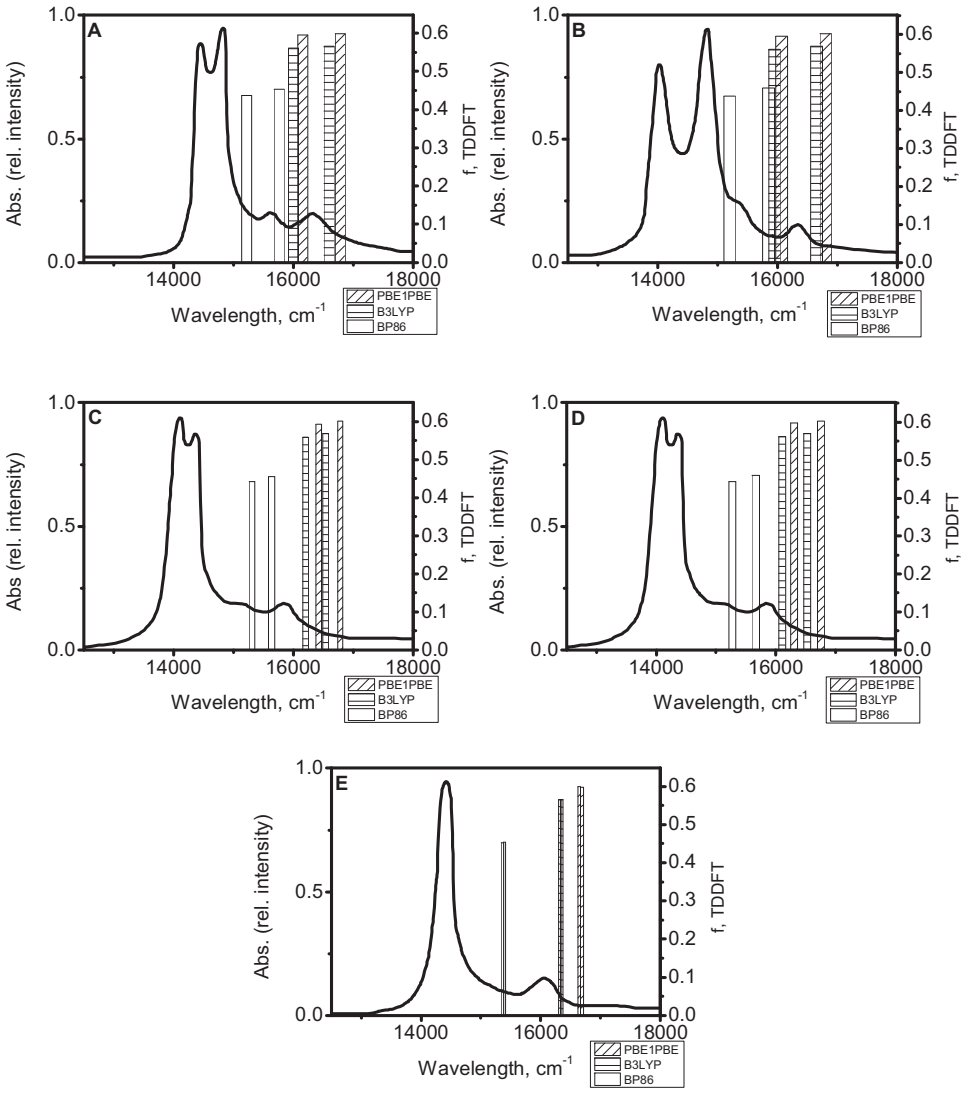

Fig. 7. Experimental UV–vis spectra of *Q*-band region and TDDFT-predicted vertical excitation energies using PBE1PBE, B3LYP, and BP86 exchange-correlation functionals (cyclohexane) for compounds **3** (A), **4** (B), **5** (C), **6** (D), and **7** (E).

and Q_y bands. The larger energy gap between the LUMO and LUMO + 1 may be responsible for the larger Q_x and Q_y-bands splitting. For example, among positional isomers **12**–**15**, compound **13** has the largest LUMO–LUMO + 1 energy gap than any other isomer, so it could be expected that the *Q*-band splitting of the former would be the largest (Fig. 5). Similarly, positional isomer **11** has the largest LUMO–LUMO + 1 gap between isomers **8**–**11** and thus, it is expected that this compound will have the

Table 1
Q-band splitting energies (cm^{-1}) of compounds **1**–**15** calculated using different functionals in vacuum and different solvents.

	Sym	Exp	PBE1PBE		B3LYP		BP861			
			Vacumm	Cyclohexane	Vacumm	Cyclohexane	Vacumm	Cyclohexane	Toluene	DMSO
1	D_{4h}	0	0	0	0	0	0	0	0	0
2	C_s	278	301	369	288	355	276	323	331	369
3	C_{2v}	374	463	622	439	595	434	542	559	631
4	C_{2h}	721	602	732	576	705	563	651	668	739
5	C_{2v}	313	366	358	352	336	338	328	326	330
6	C_{2v}	313	412	441	396	417	381	391	393	428
7	C_s	0	28	45	24	40	21	32	34	47
8	C_s	–	318	386	304	372	298	350	360	391
9	C_s	–	291	347	280	335	286	324	331	365
10	C_s	–	300	362	288	349	286	332	340	375
11	C_s	–	617	657	597	635	584	599	601	637
12	C_{4h}	–	0	0	0	0	0	0	0	0
13	D_{2h}	–	759	758	723	728	716	694	690	713
14	C_s	–	379	379	364	363	360	348	346	356
15	C_{2v}	–	9	6	9	3	23	15	15	15

largest Q_x–Q_y bands splitting in UV–vis spectrum. In the case of positional isomers **3**–**7**, compound **7** has nearly degenerate LUMO and LUMO + 1 which may result in a single *Q*-band, while the largest splitting between Q_x and Q_y bands is expected for isomer **4**.

3.2. TDDFT and TDDFT-PCM calculations

Although mentioned above predictions for the Q_x and Q_y bands splitting in pyridinoporphyrazines **2**–**15** can provide a good starting point for correlation between theory and experiment, TDDFT and TDDFT-PCM calculations can provide a better quantitative description of the energetics and single-electron excitation contributions to the Q_x and Q_y bands.

In order to examine the exchange-correlation functional effect on the calculated energies and Q_x–Q_y bands splitting in pyridinoporphyrazines, TDDFT calculation were conducted using PBE1PBE, B3LYP, and BP86 functionals in vacuum, cyclohexane, toluene, and DMSO solvents. The numerical results for TDDFT and TDDFT-PCM calculations are presented in Table 1, while graphical correlations are given in Figs. 6 and S14–S15. Results for TDDFT and TDDFT-PCM of symmetric phthalocyanine **1** were discussed earlier [29] and follows the trends observed for pyridinoporphyrazines **2**–**15**. As shown in Fig. 6, all exchange-correlation functionals used in TDDFT calculations correctly predict splitting of the Q_x and Q_y bands in monopyridinoporphyrazine **2**, but slightly overestimate their energies. The absolute magnitude of the energy overestimation decreases with decreasing of amount of Hartree–Fock exchange presented in the exchange-correlation functional: PBE1PBE (25%) > B3LYP (20%) > BP86 (0%). Including solvent effect into these calculations results in a slightly better agreement between theory and experiment (Fig. 6). Calculated $Q_x - Q_y$ bands splitting of compound **2** varies between 276 and 369 cm^{-1} and is in good agreement with the experimental data for **2** (278 cm^{-1}). Different exchange-correlation functionals used in calculations do not have a profound effect on calculated $Q_x - Q_y$ band splitting with gas-phase calculations resulted in a slightly closer agreement between theory and experiment (Table 1 and Fig. S14).

TDDFT and TDDFT-PCM predicted energies and splittings of the Q_x and Q_y bands in dipyridinoporphyrazines **3**–**7** also correlate well with the available experimental data and previous tentative assignments. Sakamoto et al. [25] were able to separate four out of five possible positional isomers of such dipyridinoporphyrazines. One fraction had a relatively large $Q_x - Q_y$ bands splitting, one fraction had a single *Q*-band, and two fractions had a small $Q_x - Q_y$ bands splitting (Fig. 7). TDDFT and TDDFT-PCM calculations correlate very well with the experimental data. Positional isomers **3** and **4** should have the largest $Q_x - Q_y$ band splitting, isomers **5** and **6** should have smaller $Q_x - Q_y$ band splitting, and isomer **7** should have a single *Q*-band. Thus, TDDFT and TDDFT-PCM approach can be helpful in identification of the positional isomers of dipyridinoporphyrazines **3**–**7**.

According to the theoretical calculations, the identification of the experimentally unknown positional isomers of tripyridinoporphyrazines **8**–**11** could be significantly more challenging because compounds **8**–**10** should have very similar $Q_x - Q_y$ band splitting. Isomer **11**, however, should have a relatively large $Q_x - Q_y$ band splitting and thus can be easily identified if purified as individual isomer. Finally, although separation of the positional isomers in tetrapyridinoporphyrazines have never been specifically targeted, reported UV–vis spectra on the mixture of isomers **12**–**15** are quite different [37,48,49] and, probably, indicative of the specific dominant isomer, which can be preferentially formed under the reaction conditions. For instance, Nyokong [48] reported UV–vis spectra of tetrapyridinoporphyrazines without Q_x–Q_y bands splitting, while UV–vis spectra of the same compound reported by Sakamoto [37] and Stillman [49] have significantly splitting between Q_x and Q_y bands. Again, TDDFT and TDDFT-PCM calculations can be helpful in the identification of the positional isomers of tetrapyridinoporphyrazines **12**–**15**. Indeed, the C_{4h} symmetry of isomer **12** dictates that the only single *Q*-band must be present in UV–vis spectrum and this is also true for isomer **15** in which the LUMO and LUMO + 1 are nearly degenerate. Similarly, it is expected that the D_{2h} symmetry isomer **13** should have the largest splitting between Q_x and Q_y bands and its calculated splitting correlates very well with the *Q* band region of the UV–vis spectrum. Finally, TDDFT and

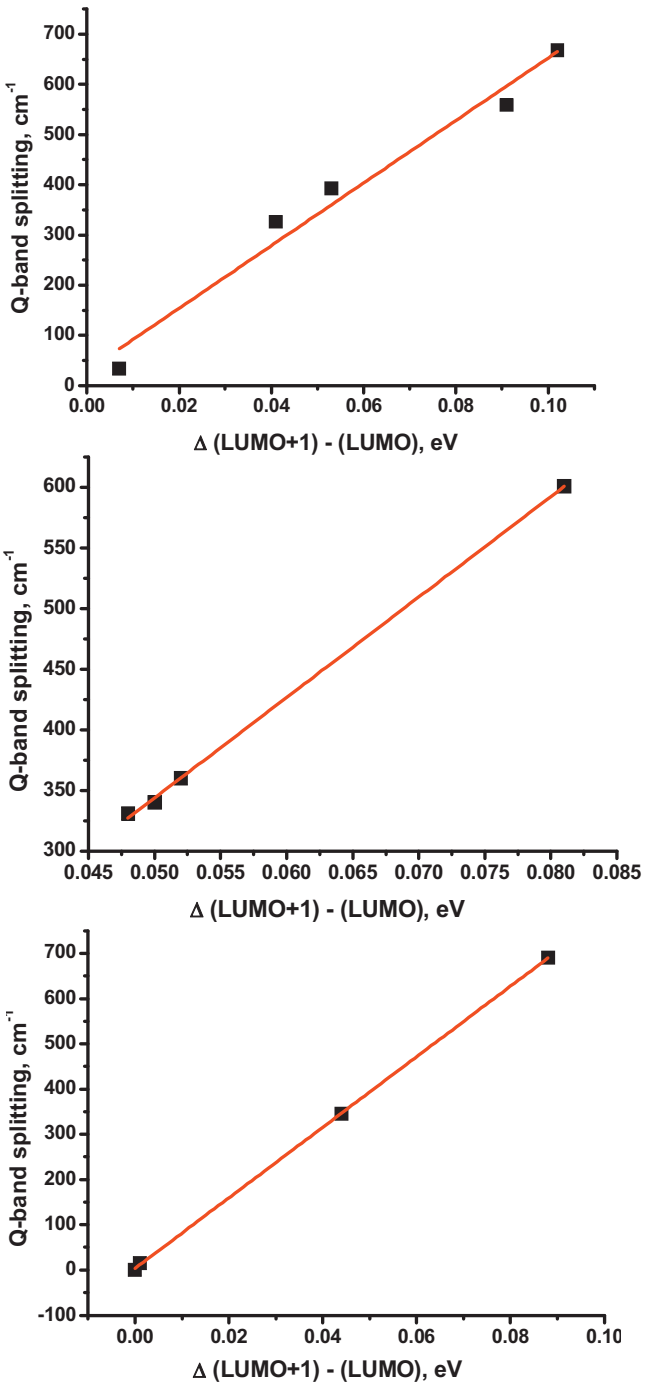

Fig. 8. Linear correlation between *Q*-band splitting energy and LUMO to LUMO + 1 energy gap for isomers **3**–**7** (top), **8**–**11** (middle) and **12**–**15** (bottom) calculated using BP86 exchange-correlation functional in toluene.

TDDFT-PCM predicts that the positional isomer **14** should have a small $Q_x - Q_y$ bands splitting.

All excited states, which correspond to the Q band region of compounds **2**–**15** can be assigned as Pc core-centered π–π^* transitions originating from the HOMO to LUMO and HOMO to LUMO + 1 excitations. Not surprisingly, and in agreement with the molecular orbital analysis, Q_x–Q_y band splitting linearly correlates with the LUMO–LUMO + 1 energy gap: the larger the LUMO–LUMO + 1 energy gap, the larger Q_x–Q_y bands splitting, as shown in Fig. 8.

4. Conclusion

The electronic structures and vertical excitation energies of fourteen pyridinoporphyrazines have been calculated using DFT, TDDFT, and TDDFT-PCM approaches using PBE1PBE, B3LYP, and BP86 exchange-correlation functionals in vacuum, cyclohexane, toluene, and DMSO. All Q_x and Q_y bands calculated were assigned as Pc core-centered π–π^* transitions, predominantly originating from the HOMO to LUMO and HOMO to LUMO + 1 excitations. TDDFT and TDDFT-PCM calculations show that Q_x–Q_y band splitting for the individual positional isomers linearly correlate with the LUMO to LUMO + 1 energy gap. A high accuracy of the predicted energies and splitting of Q_x and Q_y bands in pyridinoporphyrazines allows their assignment to known positional isomers and prediction of UV–vis spectra for the unknown individual positional isomers of pyridinoporphyrazines.

Acknowledgements

Generous support from the NSF CHE-1110455 and Minnesota Supercomputing Institute to VN are greatly appreciated. This work was also partially supported by National Natural Science Foundation of China (Grant No. 20807037) and Zhejiang Provincial Natural Science Foundation of China (Grant No. LY12B07010). We wish to acknowledge Prof. Sakamoto and Prof. Lukyanets for UV–vis spectra of selected porphyrazines.

Appendix A. Supplementary data

Supplementary data associated with this article can be found, in the online version, at http://dx.doi.org/10.1016/j.jmgm.2013.03.002.

References

[1] (a) C.C. Leznoff, A.B.P. Lever, Phthalocyanines: Properties and Applications, vol. 1–4, VCH Publishers Ltd., Cambridge, 19891993;
(b) G. de la Torre, C.G. Claessens, T. Torres, Phthalocyanines: old dyes, new materials, putting color in nanotechnology, Chemical Communications 20 (2007) 2000–2015;
(c) V.N. Nemykin, E.A. Lukyanets, The key role of peripheral substituents in the chemistry of phthalocyanines, in: K.K. Kadish, K.M. Smith, R. Guilard (Eds.), Handbook of Porphyrin Science, vol. 3, World Scientific, Singapore, 2010, pp. 1–323;
(d) E.A. Lukyanets, V.N. Nemykin, The key role of peripheral substituents in the chemistry of phthalocyanines and their analogues, Journal of Porphyrins Phthalocyanines 14 (2010) 1–40;
(e) V.N. Nemykin, E.A. Lukyanets, Synthesis of substituted phthalocyanines, ARKIVOC, (i) (2010) 136–208.

[2] (a) P. Turek, P. Petit, J.J. Andre, J. Simon, R. Even, B. Boudjema, G. Guillaud, M. Maitrot, A new series of molecular semiconductors: phthalocyanine radicals, Journal of the American Chemical Society 109 (17) (1987) 5119–5122;
(b) Y. Vertsimakha, S. Mamykin, P. Lutsyk, Substitution of phthalocyanines affecting the properties of their films and heterostructures, Chemical Physics 404 (2012) 16–21;
(c) H. Brinkmann, C. Kelting, S. Makarov, O. Tsaryova, G. Schnurpfeil, D. Wöhrle, D. Schlettwein, Fluorinated phthalocyanines as molecular semiconductor thin films, Physica Status Solidi (a) 205 (3) (2008) 409–420;
(d) J.P. Duarte, R.C. Vilão, H.V. Alberto, J.M. Gil, F.P. Gil, A. Weidinger, N.A. de Campos, K. Fostiropoulos, Muoniated radical states in the organic semiconductor phthalocyanine, Physical Review B 73 (7) (2006) 075209/1–075209/75209.

[3] (a) Y. Chen, W. Su, M. Bai, J. Jiang, X. Li, Y. Liu, L. Wang, S. Wang, High performance organic field-effect transistors based on amphiphilic tris (phthalocyaninato) rare earth triple-decker complexes, Journal of the American Chemical Society 127 (45) (2005) 15700–15701;
(b) C.F. van Nostrum, S.J. Picken, A.J. Schouten, R.J. Nolte, Synthesis and supramolecular chemistry of novel liquid crystalline crown ether-substituted phthalocyanines: toward molecular wires and molecular ionoelectronics, Journal of the American Chemical Society 117 (40) (1995) 9957–9965;
(c) J. Simon, C. Sirlin, Mesomorphic molecular materials for electronics, optoelectronics, iono-electronics: octaalkyl-phthalocyanine derivatives, Pure and Applied Chemistry 61 (1989) 1625–1629;
(d) C. Hamann, M. Hietschold, A. Mrwa, M. Mueller, M. Starke, R. Kilper, Phthalocyanine thin films for molecular electronics, Molecular Electronics 7 (1991) 129–138;
(e) D. Dini, M. Barthel, T. Schneider, M. Ottmar, S. Verma, M. Hanack, Phthalocyanines and related compounds as switchable materials upon strong irradiation: the molecular engineering behind the optical limiting effect, Solid State Ionics 165 (1) (2003) 289–303;
(f) H. Lee, J. Lee, K. Jeong, Y. Yi, J.H. Lee, J.W. Kim, S.W. Cho, Hole Injection enhancements of a CoPc and CoPc: NPB mixed layer in organic light-emitting devices, The Journal of Physical Chemistry C 116 (24) (2012) 13210–13216.

[4] (a) M.B.M. Krishna, L. Giribabu, D.N. Rao, Ultrafast third order nonlinear optical properties of water soluble zinc–octacarboxy–phthalocyanine, Journal of Porphyrins and Phthalocyanines 16 (9) (2012) 1015–1023;
(b) G. de la Torre, P. Vázquez, F. Agulló López, T. Torres, Role of structural factors in the nonlinear optical properties of phthalocyanines and related compounds, Chemical Reviews 104 (9) (2004) 3723–3750.

[5] (a) J. Marino, M.C. García Vior, L.E. Dicelio, L.P. Roguin, J. Awruch, Photodynamic effects of isosteric water-soluble phthalocyanines on human nasopharynx KB carcinoma cells, European journal of medicinal chemistry 45 (9) (2010) 4129–4139;
(b) C. Fabris, M. Soncin, G. Miotto, L. Fantetti, G. Chiti, D. Dei, D. Donata, R. Gabrio, G. Jori, Zn (II)-phthalocyanines as phototherapeutic agents for cutaneous diseases, photosensitization of fibroblasts and keratinocytes, Journal of Photochemistry and Photobiology B: Biology 83 (1) (2006) 48–54;
(c) J. Wang, H.Y. Tang, W.L. Yang, J.Y. Chen, Aluminum phthalocyanine and gold nanorod conjugates: the combination of photodynamic therapy and photothermal therapy to kill cancer cells, Journal of Porphyrins and Phthalocyanines 16 (7/8) (2012) 802–808;
(d) L. Bai, J. Guo, F.A. Bontempo III, J.L. Eiseman, The relationship of phthalocyanine 4 (Pc 4) concentrations measured noninvasively to outcome of Pc 4 photodynamic therapy in mice, Photochemistry and Photobiology 85 (4) (2009) 1011–1019;
(e) V.N. Nemykin, V.M. Mytsyk, S.V. Volkov, N. N Kobayashi, Synthesis and spectroscopic properties of new phthalocyanine complexes with potentially combined photodynamic activity and cytotoxicity for photodynamic therapy, Journal of Porphyrins and Phthalocyanines 4 (2000) 551–554.

[6] C.K. Jang, J.Y. Jaung, Electrochemical, spectroelectrochemical and ESR spectroscopic characterization of 2,3- and 3,4-cobalt tetrapyridoporphyrazine isomers in non-aqueous media, Journal of Porphyrins and Phthalocyanines 13 (8/9) (2009) 939–948.

[7] J. Shao, J. Commodore, B. Han, C. Pruente, C.A. Hansen, Electrochemical, spectroelectrochemical and ESR spectroscopic characterization of 2,3- and 3,4-cobalt tetrapyridoporphyrazine isomers in non-aqueous media, Journal of Porphyrins and Phthalocyanines 13 (8/9) (2009) 876–888.

[8] W.S. Szulbinski, J.R. Kincaid, Synthesis and spectroscopic characterization of zinc tetra (3,4-pyridine) porphyrazine entrapped within the supercages of Y-zeolite, Inorganic Chemistry 37 (19) (1998) 5014–5020.

[9] S. Palacin, A. Ruaudel-Teixier, A. Barraud, Chemical reactivity in monolayers: study of an amphiphilic tetrapyridinoporphyrazine in Langmuir-Blodgett films, The Journal of Physical Chemistry 90 (23) (1986) 6237–6242.

[10] X.S. Feng, M.X. Yu, H.G. Liu, D.J. Qian, J. Mu, Studies on the composite Langmuir-Blodgett films of tetracationic porphyrazine cobalt and methyl orange, Langmuir 16 (24) (2000) 9385–9389.

[11] T.D. Smith, J. Livorness, H. Taylor, J.R. Pilbrow, G.R. Sinclair, Physico-chemical study of copper (II) and cobalt (II) chelates of tetra-2,3-pyridinoporphyrazine, Journal of Chemical Society, Dalton Transactions 7 (1983) 1391–1400.

[12] (a) S. Moeno, M. Idowu, T. Nyokong, Spontaneous charge transfer between zinc tetramethyl-tetra-2,3-pyridinoporphyrazine and CdTe and ZnS quantum dots, Inorganica Chimica Acta 361 (9) (2008) 2950–2956;
(b) M.C. Richoux, Z.M. Abou-Gamra, Redox properties of zinc (II) tetra-N-methyl-2,3-pyridinoporphyrazine in aqueous solution, Inorganica Chimica Acta 118 (2) (1986) 115–118;
(c) P. Maillard, P. Krausz, C. Giannotti, S. Gaspard, Photoinduced activation of molecular oxygen by various porphyrins, bis-porphyrins, phthalocyanines, pyridinoporphyrazins, and their metal derivatives, Journal of Organometallic Chemistry 197 (3) (1980) 285–290.

[13] (a) C. Martí, S. Nonell, M. Nicolau, T. Torres, Photophysical properties of neutral and cationic tetrapyridinoporphyrazines, Photochemistry and Photobiology 71 (1) (2000) 53–59;
(b) E.A. Dupouy, D. Lazzeri, E.N. Durantini, Photodynamic activity of cationic and non-charged Zn (II) tetrapyridinoporphyrazine derivatives: biological consequences in human erythrocytes and *Escherichia coli*, Photochemistry and Photobiological Science 3 (11/12) (2004) 992–998.

[14] (a) T.G. Gantchev, H. Ali, J.E. van Lier, Interactions of chloroaluminum tetramethyltetrapyridinoporphyrazine with DNA, European Journal of Biochemistry 217 (1) (1993) 371–376;
(b) A. Mozaffar, S. Elham, R. Bijan, H. Leila, Thermodynamic and spectroscopic study on the binding of cationic Zn (II) and Co (II) tetrapyridinoporphyrazines to calf thymus DNA: the role of the central metal in binding parameters, New Journal of Chemistry 28 (2004) 1227–1234;
(c) A. Mozaffar, S. Elham, R. Bijan, H. Leila, A study on the binding of two water-soluble tetrapyridinoporphyrazinato copper(II) complexes to DNA, Journal of Molecular Structure 754 (2005) 116–123;
(d) A. Mozaffar, B. Abdol-Khalegh, S. Elham, G. Jahanbakhsh, Interaction of some water-soluble metalloporphyrazines with human serum albumin, Journal of Molecular Structure 705 (2004) 41–47.
[15] (a) V. Batista, M.R. Lanza, I.L. Dias, S.M. Tanaka, A.A. Tanaka, M.D. Sotomayor, Electrochemical sensor highly selective for estradiol valerate determination based on a modified carbon paste with iron tetrapyridinoporphyrazine, Analyst 133 (12) (2008) 1692–1699;
(b) Y.H. Tse, P. Janda, A.B.P. Lever, Electrode with electrochemically deposited N,N′,N″,N‴-tetramethyltetra-3,4-pyridinoporphyrazinocobalt (I) for detection of sulfide ion, Analytical Chemistry 66 (3) (1994) 384–390;
(c) Z. Xu, G. Zhang, Z. Cao, J. Zhao, H. Li, Effect of *N* atoms in the backbone of metal phthalocyanine derivatives on their catalytic activity to lithium battery, Journal of Molecular Catalysis A: Chemical 318 (1) (2010) 101–105;
(d) T.P. Umile, D. Wang, J.T. Groves, Dissection of the mechanism of manganese porphyrin-catalyzed chlorine dioxide generation, Inorganic Chemistry 50 (20) (2011) 10353–10362;
(e) D. Wöhrle, J. Gitzel, I. Okura, S. Aono, Photoredox properties of tetra-2,3-pyridinoporphyrazines (29H 31H-tetrapyrido[2,3-b:2′,3′-g:2″,3″-l:2,3-q] porphyrazine), Journal of the Chemical Society, Perkin Transactions 2 (8) (1985) 1171–1178.
[16] R.P. Linstead, E.G. Noble, J.M. Wright, Phthalocyanines. IX. Derivatives of thiophene, thionaphthene, pyridine and pyrazine, and a note on the nomenclature, Journal of the Chemical Society (1937) 911–921.
[17] M. Yokote, F. Shibamiya, S. Tokairin, Sakae, Aza compounds. XXVII. Copper phthalocyanine nitrogen isolog (copper tetra-3,4-pyridinoporphyrazine) synthesized from cinchomeronic acid, Kogyo Kagaku Zasshi 67 (1964) 166–168.
[18] M. Yokote, F. Shibamiya, H. Hayakawa, Aza compounds. XXIX, Yuki Gosei Kagaku Kyokaishi 23 (1965) 151–155.
[19] M. Yokote, F. Shibamiya, Cu Bz–azaphthalocyanine, Kogyo Kagaku Zasshi Zasshi 62 (1959) 224–227.
[20] M. Hanack, R. Thies, [Tetra(2,3-pyrido)porphyrazinato]iron(II) compounds with isocyanides as axial ligands, Chemische Berichte-Recueil 121 (7) (1988) 1225–1230.
[21] S. Tokita, M. Kojima, N. Kai, K. Kuroki, H. Tomoda, S. Saitoh, S. Shiraishi, Synthesis and properties of 2, 3,9,10,16,17,23,24-octaalkyltetrapyrazinoporphyrazines, Nippon Kagaku Kaishi (1990) 219–224.
[22] K. Sakamoto, T. Kato, E. Ohno-Okumura, M. Watanabe, M.J. Cook, Synthesis of novel cationic amphiphilic phthalocyanine derivatives for next generation photosensitizer using photodynamic therapy of cancer, Dyes and Pigments 64 (1) (2005) 63–71.
[23] C. Ramirez, C. Antonacci, J. Ferreira, R.D. Sheardy, The Facile Synthesis and characterization of novel cationic metallated and nonmetallated tetrapyridino porphyrazines having different metal centers, Synthetic Communications 34 (18) (2004) 3373–3379.
[24] M.J. Danzig, C.Y. Liang, E. Passaglia, Preparation and electrical conductivity of copper tetra-2,3-pyridinoporphyrazine and copper tetra-2,3-pyrazinoporphyrazine, Journal of the American Chemical Society 85 (6) (1963) 668–671.
[25] K. Sakamoto, T. Kato, M.J. Cook, Position isomer separation of non-peripheral substituted zinc dibenzo-di(3,4-pyrido)porphyrazines, Journal of Porphyrins and Phthalocyanines 5 (10) (2001) 742–750.
[26] M.J. Cook, A. Jafari-Fini, Pyridino [34] tribenzoporphyrazines: edge-to facd versus face-to face assemblies among phthalocyanine analogues, Journal of Materials Chemistry 7 (12) (1997) 2327–2329.
[27] K. Ishii, S. Abiko, M. Fujitsuka, O. Ito, N. Kobayashi, Exciton interactions in a self-assembled phthalocyanine dimmer, Journal of the Chemical Society, Dalton Transactions 8 (2002) 1735–1739.
[28] (a) M.J. Gouterman, in: D. Dolphin (Ed.), The Porphyrins, vol. III, Academic Press, New York, 1978, pp. 1–165;
(b) P.G. Seybold, M.J. Gouterman, Porphyrins: XIII: fluorescence spectra and quantum yields, Journal of Molecular Spectroscopy 31 (1) (1969) 1–13;
(c) M.J. Gouterman, Spectra of porphyrins, Journal of Molecular Spectroscopy 6 (1961) 138–163.
[29] V.N. Nemykin, R.G. Hadt, R.V. Belosludov, H. Mizuseki, Y. Kawazoe, Influence of molecular geometry, exchange-correlation functional, and solvent effects in the modeling of vertical excitation energies in phthalocyanines using time-dependent density functional theory (TDDFT) and polarized continuum model TDDFT methods: can modern computational chemistry methods explain experimental controversies? Journal of Physical Chemistry A 50 (111) (2007) 12901–12913.
[30] Y. Muranaka, M. Matsumoto, J.Z. Uchiyama, Y.Z. Jiang, A. Bian, N. Ceulemans, Kobayashi, Definitive assignments of the visible-near-IR bands of porphyrin-naphthalocyanine rare-earth sandwich double- and triple-decker compounds by magnetic circular dichroism spectroscopy, Inorganic Chemistry 44 (11) (2005) 3818–3826.
[31] J. Mack, M.J. Stillman, Assignment of the optical spectra of metal phthalocyanines through spectral band deconvolution analysis and ZINDO calculations, Coordination Chemistry Reviews 221 (2001) 993–1032.
[32] S. Sripothongnak, C.J. Ziegler, M.R. Dahlby, V.N. Nemykin, Controllable and reversible inversion of the electronic structure in nickel N-confused porphyrin: a case When MCD matters, Inorganic Chemistry 50 (2011) 6902–6909.
[33] V.N. Nemykin, J.R. Sabin, Profiling energetics and spectroscopic signatures in prototropic tautomers of asymmetric phthalocyanine analogues, The Journal of Physical Chemistry A 116 (27) (2012) 7364–7371.
[34] Y.L. Gao, P.V. Solntsev, V.N. Nemykin, Comparative electronic structures and UV–vis spectra of tribenzosubporphyrin, tribenzomonoazasubporphyrin, tribenzodiazasubporphyrin, and subphthalocyanine: insight from DFT and TDDFT calculations, Journal of Molecular Graphics and Modelling 38 (2012) 369–374.
[35] L.J. Zhang, D.D. Qi, L.Y. Zhao, Y.Z. Bian, W.J. Li, Substituent effects on the structure-property relationship of unsymmetrical methyloxy and methoxycarbonyl phthalocyanines: DFT and TDDFT theoretical studies, Journal of Molecular Graphics and Modelling 35 (2012) 57–65.
[36] Y.L. Yang, L.S. Guo, Q.Q. Chen, H.F. Sun, J. Liu, X.X. Zhang, X. Pan, S.Y. Dai, Theoretical design and screening of panchromatic phthalocyanine sensitizers derived from TT1 for dye-sensitized solar cells, Journal of Molecular Graphics and Modelling 34 (2012) 1–9.
[37] K. Sakamoto, T. Kato, T. Kawaguchi, E. Ohno-Okumura, T. Urano, T. Yamaoka, S.M.J. Suzuki, Cook Photosensitizer efficacy of non-peripheral substituted alkylbenzopyridoporphyrazines for photodynamic therapy of cancer, Journal of Photochemistry and Photobiology A: Chemistry 153 (1) (2002) 245–253.
[38] A.D. Becke, Density-functional exchange-energy approximation with correct asymptotic behavior, Physical Review A 38 (1988) 3098–3100.
[39] J.P. Perdew, Density functional approximation for the correlation energy of the inhomogeneous electron gas, Physical Review B 33 (1986) 8822–8824.
[40] J.P. Perdew, K. Burke, M. Ernzerhof, Generalized gradient approximation made simple, Physical Review Letters 77 (1996) 3865–3868.
[41] J.P. Perdew, K. Burke, M. Ernzerhof, Errata: generalized gradient approximation made simple, Physical Review Letters 78 (1997) 1396.
[42] A.D. Becke, Density-functional exchange-energy approximation with correct asymptotic-behavior, Physical Review A 38 (1988) 3098–3100.
[43] J.P. Perdew, Density-functional approximation for the correlation energy of the inhomogeneous electron gas, Physical Review B 33 (1986) 8822–8824.
[44] V.A. Rassolov, J.A. Pople, M.A. Ratner, T. L, Windus, 6-31G* basis set for atoms K through Zn, The Journal of chemical physics 109 (1998) 1223–1229.
[45] (a) M.M. Francl, W.J. Pietro, W.J. Hehre, J.S. Binkley, D.J. DeFrees, J.A. Pople, M.S. Gordon, Self-consistent molecular orbital methods. 23. A polarization-type basis set for 2nd-row elements, The Journal of Chemical Physics 77 (1982) 365436–365465;
(b) A.D. McLean, G.S. Chandler, Contracted Gaussian basis sets for molecular calculations. I. Second row atoms, $Z = 11–18$, The Journal of Chemical Physics 72 (1980) 5639–5648.
[46] (a) M. Caricato, B. Mennucci, J. Tomasi, F. Ingrosso, R. Cammi, S. Corni, G. Scalmani, Formation and relaxation of excited states in solution: a new time dependent polarizable continuum model based on time dependent density functional theory, The Journal of Chemical Physics 124 (2006) 124520–124532;
(b) V. Barone, M. Cossi, J. Tomasi, Geometry optimization of molecular structures in solution by the polarizable continuum model, Journal of Computational Chemistry 19 (1998) 404–417;
(c) B. Mennucci, J. Tomasi, Continuum solvation models: a new approach to the problem of solute's charge distribution and cavity boundaries, The Journal of Chemical Physics 106 (1997) 5151–5158.
[47] M.J. Frisch, G.W. Trucks, H.B. Schlegel, G.E. Scuseria, M.A. Robb, J.R. Cheeseman, G. Scalmani, V. Barone, B. Mennucci, G.A. Petersson, H. Nakatsuji, M. Caricato, X. Li, H.P. Hratchian, A.F. Izmaylov, J. Bloino, G. Zheng, J.L. Sonnenberg, M. Hada, M. Ehara, K. Toyota, R. Fukuda, J. Hasegawa, M. Ishida, T. Nakajima, Y. Honda, O. Kitao, H. Nakai, T. Vreven, J.A. Montgomery Jr., J.E. Peralta, F. Ogliaro, M. Bearpark, J.J. Heyd, E. Brothers, K.N. Kudin, V.N. Staroverov, R. Kobayashi, J. Normand, K. Raghavachari, A. Rendell, J.C. Burant, S.S. Iyengar, J. Tomasi, M. Cossi, N. Rega, J.M. Millam, M. Klene, J.E. Knox, J.B. Cross, V. Bakken, C. Adamo, J. Jaramillo, R. Gomperts, R.E. Stratmann, O. Yazyev, A.J. Austin, R. Cammi, C. Pomelli, J.W. Ochterski, R.L. Martin, K. Morokuma, V.G. Zakrzewski, G.A. Voth, P. Salvador, J.J. Dannenberg, S. Dapprich, A.D. Daniels, O. Farkas, J.B. Foresman, J.V. Ortiz, J. Cioslowski, D.J. Fox, Gaussian 09, Gaussian Inc., Wallingford, CT, 2009.
[48] I. Seotsanyana-Mokhosi, N. Kuznetsova, T. Nyokong, Photochemical studies of tetra-2,3-pyridinoporphyrazines, Journal of Photochemistry and Photobiology A: Chemistry 140 (3) (2001) 215–222.
[49] E.A. Ough, M.J. Stillman, K.A. Creber, Absorption and magnetic circular dichroism spectra of nitrogen homologues of magnesium and zinc phthalocyanine, Canadian Journal of Chemistry 71 (11) (1993) 1898–1909.